A thin-film multichannel electrode for muscle recording and stimulation in neuroprosthetics applications

Muceli, Silvia; Poppendieck, Wigand; Hoffmann, Klaus-Peter; Dosen, Strahinja; León, Julián Benito; Barroso, Filipe O; Pons, José Luis; Farina, Dario

Published in:
Journal of Neural Engineering

DOI (link to publication from Publisher):
10.1088/1741-2552/ab047a

Publication date:
2019

Document Version
Publisher's PDF, also known as Version of record

A thin-film multichannel electrode for muscle recording and stimulation in neuroprosthetics applications

OPEN ACCESS
IOP Publishing

Made open access 10 April 2019
Journal of Neural Engineering

J. Neural Eng. **16** (2019) 026035 (10pp)
https://doi.org/10.1088/1741-2552/ab047a

A thin-film multichannel electrode for muscle recording and stimulation in neuroprosthetics applications

Silvia Muceli[1], Wigand Poppendieck[2], Klaus-Peter Hoffmann[3], Strahinja Dosen[4], Julián Benito-León[5,6,7], Filipe Oliveira Barroso[8], José Luis Pons[8] and Dario Farina[1,9]

[1] Department of Bioengineering, Imperial College London, London, United Kingdom
[2] Mannheim University of Applied Sciences, Mannheim, Germany
[3] Department of Medical Engineering and Neuroprosthetics, Fraunhofer Institute for Biomedical Engineering, St Ingbert, Germany
[4] Department of Health Science and Technology, Center for Sensory-Motor Interaction, Aalborg University, Aalborg, Denmark
[5] Department of Neurology, University Hospital 12 de Octubre, Madrid, Spain
[6] Center of Biomedical Network Research on Neurodegenerative diseases (CIBERNED), Madrid, Spain
[7] Faculty of Medicine, Department of Medicine, Complutense University, Madrid, Spain
[8] Neural Rehabilitation Group, Cajal Institute, Spanish National Research Council (CSIC), Madrid, Spain

E-mail: d.farina@imperial.ac.uk

Received 28 November 2018, revised 21 January 2019
Accepted for publication 5 February 2019
Published 27 February 2019

Abstract

Objective. We propose, design and test a novel thin-film multichannel electrode that can be used for both recording from and stimulating a muscle in acute implants. *Approach*. The system is built on a substrate of polyimide and contains 12 recording and three stimulation sites made of platinum. The structure is 420 μm wide, 20 μm thick and embeds the recording and stimulation contacts on the two sides of the polyimide over an approximate length of 2 cm. We show representative applications in healthy individuals as well as tremor patients. The designed system was tested by a psychometric characterization of the stimulation contacts in six tremor patients and three healthy individuals determining the perception threshold and current limit as well as the success rate in discriminating elicited sensations (electrotactile feedback). Also, we investigated the possibility of using the intramuscular electrode for reducing tremor in one patient by electrical stimulation delivered with timing based on the electromyographic activity recorded with the same electrode. *Main results*. In the tremor patients, the current corresponding to the perception threshold and the current limit were 0.7 ± 0.2 and 1.4 ± 0.7 mA for the wrist flexor muscles and 0.4 ± 0.2 and 1.5 ± 0.7 mA for the extensors. In one patient, closed-loop stimulation resulted in a decrease of the tremor power >50%. In healthy individuals the perception threshold and current limits were 0.9 ± 0.6 and 2.1 ± 0.6 mA for the extensor carpi radialis muscle. The subjects could distinguish four or six stimulation patterns (two or three stimulation sites $\times$ two stimulation current amplitudes) with true positive rate >80% (two subjects) and >60% (one subject), respectively. *Significance*. The proposed electrode provides a compact multichannel interface for recording electromyogram and delivering electrical stimulation in applications such as neuroprostheses for tremor suppression and closed-loop myoelectric prostheses.

[9] Department of Bioengineering, Imperial College of Science, Technology and Medicine, London SW7 2AZ, United Kingdom.

Keywords: intramuscular electrode, neuroprosthesis, electrical stimulation, tremor, sensory feedback

(Some figures may appear in colour only in the online journal)

1. Introduction

In rehabilitation engineering, muscle recordings are commonly used to access the neural drive of movement while electrical stimulation is applied to elicit afferent feedback. For instance, in myoelectric prostheses, electromyographic (EMG) signals are detected for inferring which movement an amputee intends to perform (feedforward control) (Asghari Oskoei and Hu 2007). Commercial prostheses are operated by feedforward commands but an ideal artificial replacement of the upper limb would require the restoration of both motor and sensory function. Artificial feedback can be provided via electrical or mechanical stimulation that the subject is trained to associate to the state of the prosthesis (e.g. aperture and grasping force) (Antfolk *et al* 2013). Electrical stimulation has been also used in neuroprostheses for tremor suppression (Prochazka *et al* 1992, Gallego *et al* 2013). In a previous study (Dosen *et al* 2015), we proposed a strategy that detects tremor from the electromyographic signals of the muscles originating tremor and counteracts it by applying out-of-phase electrical stimulation to the same muscles.

The aforementioned studies relied on surface recording and stimulation. This is a common procedure due to the non-invasiveness and easy placement of the electrodes. However, only superficial muscles can be accessed using surface electrodes. Moreover, with surface electrodes it may be more difficult to achieve a stable connection with the biological tissue (due for instance to electrode lift-off) which may result in noisy measurements and/or signal loss during recording and non-uniform current delivery during stimulation. Invasive electrodes on the other hand can be implanted in deep muscles and they provide a direct and tight contact with the muscles, bypassing the superficial layers of adipose and connective tissue and thereby improving the quality of recording and stimulation. Also, invasive solutions may be preferred to avoid daily electrode repositioning and make the neuroprosthesis less visible to the user and other individuals providing a better aesthetic result.

Invasive solutions usually interface the electrodes with the brain (Maynard, Nordhausen and Normann 1997, Heuschkel *et al* 2002) or nerves (Lago *et al* 2007, Rossini *et al* 2010, Raspopovic *et al* 2014). Placing the electrode next or around a nerve or implanting it in the brain requires a surgical procedure. Some subjects, such as amputees, may be reluctant to undergo an additional surgery. Therefore, in some applications the muscle may be a preferable alternative for implants, accessible with relatively less invasive procedures. For example, intramuscular electrodes can be placed within a muscle using a hypodermic needle (Cipriani *et al* 2014). However, these electrodes typically include a single contact point and therefore, several electrodes need to be inserted for multichannel recording/stimulation. Invasive electrodes for epimysial muscle recording and stimulation have been recently proposed but they have been tested only in animal preparations (Guo *et al* 2009, Guvanasen *et al* 2017, Muceli *et al* 2019). In all these cases, the individual electrodes are dedicated to either stimulation or recording.

In previous studies we have proposed and tested multichannel electrodes for EMG recordings made of a thin-film of polyimide (Muceli *et al* 2015, 2019, Luu *et al* 2018). In this study, we propose a novel intramuscular electrode based on thin-film technology that includes multiple contacts for both detection and stimulation in the same polyimide substrate. The main drawback of invasive electrodes is that they are implanted through a surgical procedure, therefore their use is justified only if they provide comparable or superior performance than the surface counterpart. This poses challenges in the electrode design that has to be refined to the highest level possible before implantation. The electrode presented herein has been designed for acute invasive recording/stimulation experiments. As done with classic intramuscular wires (Basmajian and Stecko 1962), the electrode is driven into a muscle with a standard hypodermic needle, withdrawn after the insertion. In this way, the system can be used for acute experiments and the design iteratively refined before producing a fully implantable solution. We herein describe the design and report some representative examples of *in vivo* applications in humans in the neuroprosthetics field. The examples include both stimulation and recording, with main emphasis on the stimulation capabilities since recording with similar electrode sites has been previously shown (Muceli *et al* 2015, Negro *et al* 2016, Luu *et al* 2018).

2. Methods

2.1. Electrode design and manufacturing

The electrode is a structure micromachined on a thin-film polyimide substrate with sites (contacts) for muscle recording and stimulation, built on the two sides of the polyimide (figure 1(A)). The structure is 20 μm thick and includes a 420 μm wide filament embedding the recording and stimulation sites (over a length of ~2 cm) and a 100 μm wide filament used for facilitating the insertion of the structure into the muscle (figure 1(D)). The design includes 12 recording sites and three stimulation sites, with areas 5257 μm^2 and 1.08 mm^2 each, respectively (figure 1(E)). The inter-site distance was 1.875 and 7.5 mm for the recording and stimulation contacts, respectively. The sites were arranged so that four recording contacts were on the opposite of each of the three stimulation contacts (figure 1(A)). The size of the stimulation sites was chosen so that stimulation pulses could be applied safely, without any irreversible reactions, which would cause corrosion and subsequent tissue damage over the long term. The charge injection capacity (amount of reversibly injectable charge) for platinum is in the range of 50–350 $\mu C\ cm^{-2}$

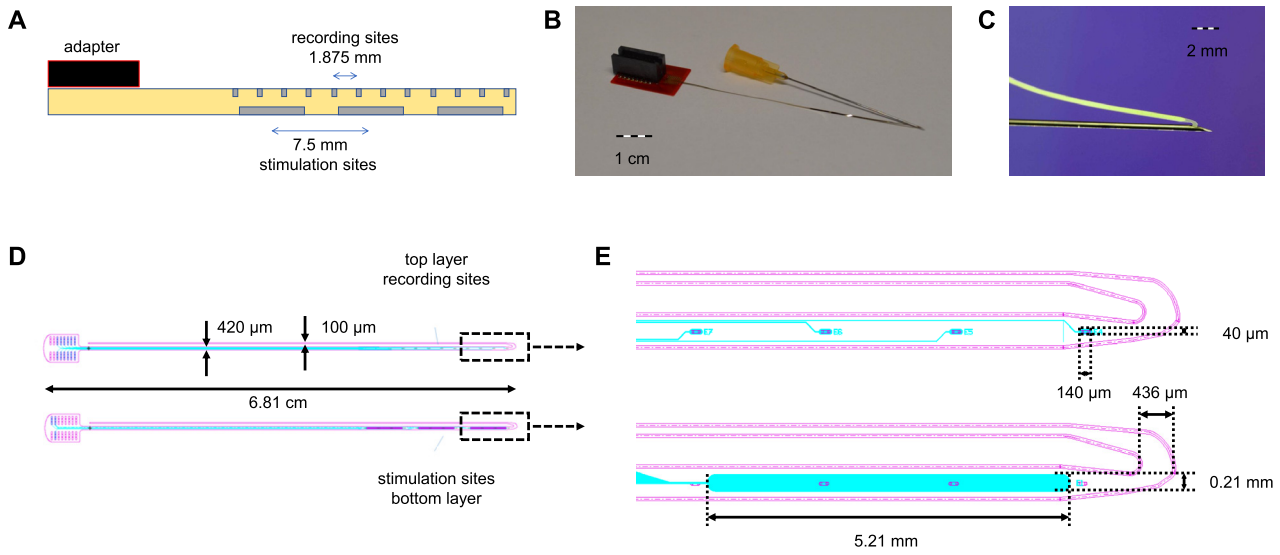

Figure 1. Design of the intramuscular thin-film electrode for recording and stimulation. ((A) Not in scale) The electrode is constituted by a polyimide substrate and embedded recording and stimulation sites on the two sides of the substrate. Electrode contacts are arranged equidistant in a linear configuration over ~2 cm at the tip of the polyimide structure. (B) A picture of the final assembly. (C) A close-up of the tip of the structure bottom layer representing a stimulation contact. (D) Top and bottom views of the thin-film electrode with the recording and stimulation sites, respectively, as removed from the wafer (i.e. before interconnection with the FR4 and adapter). (E) The detection and stimulation sites have oval shape with axes $(20 + 100 + 20)$ μm $\times$ 40 μm and $(0.105 + 5 + 0.105)$ mm $\times$ 0.21 mm, respectively.

(Rose and Robblee 1990, Cogan 2008, Poppendieck *et al* 2009). To maximize safety in human applications, the conservative value of 50 μC cm^{-2} was chosen as the basis for specifying the maximum current allowed (charge injection capacity · electrode area/pulse width) which resulted in 2.7 mA, assuming stimulation pulses of 200 μs duration.

The polyimide electrodes were produced using a double-sided manufacturing process (Poppendieck *et al* 2014). A 4-inch silicon wafer was used as platform for the production. A platinum etch mask was deposited and lift-off structured. Then, a 5 μm layer of polyimide was spun on the wafer. Platinum and gold were sputtered, and lift-off structured to form the stimulation sites and tracks. A 10 μm layer of polyimide was deposited, and then gold tracks and platinum recording sites were sputtered and lift-off structured, followed by a 5 μm polyimide layer for insulation. The backside of the silicon wafer underwent two steps of ion etching, the first to reach the stimulation contacts and the second to open them using the previously deposited platinum layer as etch mask. An aluminium etch mask was then deposited on the polyimide top side and used for reactive ion etching to open the recording contacts. Finally, the aluminium mask was removed and the electrodes peeled-off from the wafer with tweezers.

For connection with external hardware, a 16-pin connector (Harwin M50-4900845) was soldered to a custom-designed FR4 adapter attached to the polyimide structure by using the Microflex technology (Meyer *et al* 2001). Twelve pins were used for the recording contacts and three for the stimulation. The guiding filament was threaded into a hypodermic needle (25G, B. Braun AG, Melsungen, Germany) used for inserting the thin-film electrode within the muscle and withdrawn prior to experimental EMG recordings. The final assembly is shown in figure 1(B) (close-up in figure 1(C)).

To increase the effective surface area, both recording and stimulation sites were coated with microrough platinum using electroplating from an aqueous solution of hexachloroplatinic acid (Poppendieck *et al* 2014). Before and after coating, the electrode contacts were characterized by impedance spectroscopy in the frequency range of 0.1 Hz–100 kHz. Moreover, cyclic voltammetry (Vrabec *et al* 2016) was performed within a voltage range of -0.6 V and $+0.9$ V verasus Ag/AgCl at a scan rate of 100 mV s^{-1}.

After fabrication, electrodes were rinsed in isopropyl alcohol (IPA) for cleaning both before and after coating. Following electrical characterization, each electrode was tested for biocompatibility according to DIN EN ISO 10993. Tests for cytotoxicity (elution test), irritation (intracutaneous reactivity) and sensitization (local lymph node assay) were conducted by an external laboratory (MDT Medical Device Testing GmbH, Ochsenhausen, Germany). Electrodes were then sterilized with ethylene oxide gas (ETO). The ETO sterilization procedure causes less temperature/humidity stress to the electrodes compared to autoclaving. Care was taken to have a period of at least one week between sterilization and implantation, in order to ensure that no residual gas was present at the electrode.

2.2. Experiments

Two experiments were carried out to study the feasibility of using the electrodes in neuroprosthetic applications, specifically for tremor suppression and for providing sensory feedback to a user of myoelectric prostheses. All participants of the study (tremor patients and healthy individuals) were recruited from the Hospital Universitario 12 de Octubre (Madrid, Spain) where the experiments took place. The experiments were

conducted in accordance with the Declaration of Helsinki and approved by the local ethical committee. All participants signed a written informed consent before the inclusion.

2.2.1. Experiments in tremor patients. We have previously proposed a tremor reduction system that relies on EMG for detection of tremorogenic bursts and low amplitude electrical stimulation applied in counter phase to pairs of antagonist muscles for counteracting the occurrence of tremor (Dosen *et al* 2015). The system was based on surface electrodes for both recording and stimulation. In the perspective of making the system implantable, we tested the designed thin-film electrodes. Six patients (age: 61.3 $\pm$ 15.3, three women, two diagnosed with essential tremor (ET) and four with Parkinson's disease (PD)) took part in the study. For consistency with our previous study (Dosen *et al* 2015), patients exhibiting mainly flexion/extension tremor at the wrist were included in these experimental measures.

Subjects sat in front of a table during the experiment. The upper limb that was most affected by tremor was targeted. As ET patients are primarily affected by postural tremor while patients with PD exhibit tremor mainly at rest, the first group of patients were asked to hold the upper limb outstretched against gravity and the second group had the wrist resting on the support placed on a table in front of them. While patients held these positions, an experimenter identified the flexor and extensor muscles generating tremor by palpating the forearm. Electrodes were inserted at the belly of the two muscles at a depth dependent on the muscle thickness. Therefore, the number of recording/detection sites within the target muscles varied from subject to subject. A disposable oval electrode (4 cm $\times$ 6.4 cm, Pals Platinum, Axelgaard, US) was placed at the wrist to act as a common ground. EMG sampling and electrical stimulation were obtained using custom made hardware and software (a research amplifier and a stimulator produced by OT Bioelettronica, Italy). Signals were sampled at 1 kHz. The stimulation frequency was set to 75 Hz and the duration of each charged-balanced biphasic pulse was 200 μs.

For all six patients, we performed a psychometric evaluation of the electrode identifying the perception, discomfort and motor thresholds for each stimulation channel as described in the following. Using the method of limits (Kingdom and Prins 2009), the stimulation current was initially set to 0.1 mA and gradually increased in steps of 0.1 mA for each of the stimulation sites of the same multichannel electrode up to the current limit. Participants were instructed to inform the experimenter when they started to perceive the stimulus (perception threshold) and when they started perceiving the stimulus as uncomfortable (discomfort threshold). The motor threshold was defined as the minimal current that elicited a muscle contraction, as detected visually and by palpating muscles and tendons. The delivered current never exceeded 2.6 mA according to the specification of the thin-film stimulation electrodes (0.1 mA below the maximal current). The current limit was defined as the minimal current among the currents that determined the discomfort threshold, the motor threshold and the maximal current. The aim was to determine the stimulation current that elicited comfortable sensations and activated afferent fibers without recruiting motor nerves, which is required for tremor suppression through neuromodulation, as explained in Dosen *et al* (2015). The test was repeated three times and the average of the three values was taken. The procedure was repeated for the flexor and extensor muscles.

To prove the feasibility of reducing tremor with a system based on (acutely) implanted electrodes, we visually inspected the EMG and tested the stimulation in all patients. Moreover, in one of the six patients we reproduced the full experiment carried out in Dosen *et al* (2015). Briefly, we used an interleaved strategy where we alternated recording and stimulation time intervals of 1 and 2 s, respectively. Recording windows were used to calculate the tremor frequency in order to properly set the timing of the stimulation bursts in the subsequent stimulation window. A signal from the flexor or extensor muscles was used as a trigger for establishing the timing of the out-of-phase stimulation. Recording channels were visually inspected to identify those where tremor bursts were clearly visible. The best channel was selected as a trigger and identification of the tremor bursts was done by locating the peaks of the envelope of the EMG signal in the selected channel. The tremor frequency was calculated from the peaks identified in the recording window and used to time the stimulation in the subsequent stimulation window. This simple procedure was adopted in order to limit the computational burden in this real-time application, since the processing of the EMG signals and control of stimulation was performed in the embedded recording and stimulation system. In order to counteract tremor, the muscle antagonist to that used as trigger was stimulated when a tremor burst in the trigger muscle was estimated to occur (out-of-phase strategy). The amplitude of the stimulation current used through the experiment was set to $CP + 0.75 * (CL - CP)$, where CP indicates the perception threshold and CL the current limit. In this way the delivered stimulation was always at a comfortable sensory level.

To assess tremulous movements, we used a commercial inertial measurement system (XBus kit, XSens, NL) including a control box and a set of inertial units (MTx, XSens, NL) measuring the full 3D orientation of the segments to which they were attached. Two units were strapped to the dorsal sides of the forearm and hand so that the wrist flexion/extension joint angle could be computed. The unit data were acquired at 100 Hz.

Two trials of approximately 1 min each were recorded. The first 30 s were used to provide an estimate of the tremor intensity at baseline (system OFF). In the remaining 30 s the tremor suppression system was ON.

The system performance was assessed by comparing the power of the tremor signals as measured by the inertial measurement units during the intervals where the system was ON versus the intervals where the system was OFF (baseline).

We calculated the wrist joint angle because we aimed at suppressing wrist flexion/extension tremor and we targeted the corresponding muscles. The wrist angular signals were filtered in the tremor bandwidth (3 to 12 Hz) and the power spectral density was calculated using the Welch periodogram. The power was then estimated integrating the power spectral density over the tremor frequencies. Finally, the tremor suppression was calculated as $100\% \cdot (1 - PR)$ where the power ratio (PR) is the ratio of the tremor power when the system was ON versus OFF.

2.2.2. Multichannel sensory feedback. Another envisaged application of the proposed electrode is in closed-loop myoelectric control systems for prosthetic devices that rely on electrical stimulation for providing sensory feedback. The sensory information may be encoded by modulation of stimulation parameters (e.g. spatial, frequency, pulse width and amplitude or combination of them (Dosen *et al* 2015, Graczyk *et al* 2016)). In our experiment, we tested if different stimulation channels of the proposed electrode provided sensation that could be distinguished by the subject when the stimulation amplitude assumed two different values. The values were determined so that they were within the range of comfortable sensory stimulation as explained in the following. We also assessed if the subjects were able to discriminate the sensations produced by delivering stimulation at different depths in the tissue, i.e. across the three electrode contacts.

Three healthy able-bodied individuals (S1–3, one female, range 33–38 years) participated in the experiments after signing the informed consent form. The electrode was inserted in the extensor carpi radialis muscle with a depth and insertion angle such that the two deepest stimulation sites were within the muscle while the shallow site was close to the skin/adipose tissue layer. Stimulation frequency was set to 100 Hz, pulse duration to 200 μs (with charge-balanced biphasic shape), and the stimulation was delivered in 1 s bursts. A wrist band was used as ground electrode. Perception threshold and current limit were determined for each stimulation channel identically as in tremor patients (section 2.2.1). Two stimulation levels were set: low $L = CP + 0.2 * (CL - CP)$ and high $H = CP + 0.75 * (CL - CP)$, where CP indicates the current corresponding to the perception threshold and CL the current limit. The first participant was trained to recognize six stimulation patterns (three stimulation channels $\times$ two stimulation levels (L and H)), while the two remaining subjects were trained to discriminate between four stimulation patterns (two stimulation channels (one deep and one superficial) $\times$ two stimulation levels (L and H)).

As in Štrbac *et al* (2016), the training included two phases: learning and reinforced learning, and was followed by a validation phase. During each of the three phases, each pattern was presented seven times, in random order, hence 7×6 and 7×4 presentations for the first and two other participants, respectively. The time interval between presentation of the stimulation patterns was about 30 s. Five min rest were allowed after each phase. During learning, the experimenter verbally informed the subject about which pattern was presented after the stimulation. During the reinforced learning phase, the subject was asked to identify which pattern was delivered and the experimenter confirmed or corrected what the subject stated. During the validation phase, the subject identified the pattern and the experimenter annotated the subject response without providing any feedback. Results were displayed as confusion matrices. The performance was evaluated by means of the true positive rate (TPR, sensitivity) and true negative rate (TNR, specificity) defined as $TPR = TP/(TP + FN)$ and $TNR = TN/(TN + FP)$, where TP (true positive) was the number of correctly identified patterns during the testing phase, FN (false negative) and FP (false positive) the number of incorrectly identified patterns, and TN (true negative) the number of correctly 'rejected' patterns (subject choosing a different pattern when the current pattern is not the correct one).

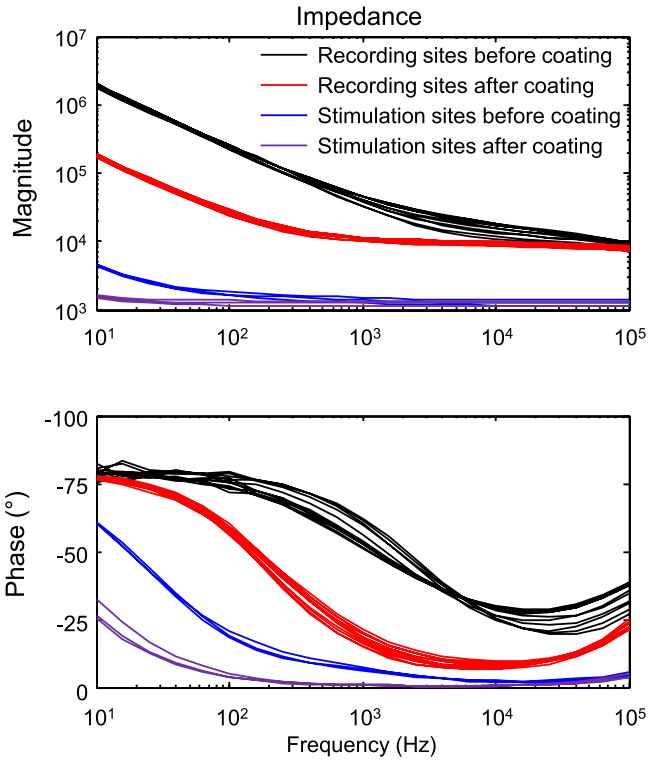

Figure 2. Representative example of the magnitude and phase of the impedance of the 12 recording sites before (black) and after (red) coating with microrough platinum and of the three stimulation sites coated (purple) and not (blue). Impedance decreased following the coating procedure.

3. Results

3.1. Impedance measurements

Figure 2 shows the impedance spectroscopy results for one of the electrodes used in the study. The impedance values are similar across recording sites and across stimulation sites. The stimulation contacts have lower impedance than the recording contacts (due to the larger area), and in both types of contacts coating with microrough platinum reduced impedance (in the low frequency range). At 1 kHz, the absolute impedance was ~100 kΩ for the uncoated recording sites, and ~10 kΩ for the contacts coated with microrough platinum. At the same frequency, the impedance of the stimulation sites was approximately 1.5 kΩ.

Figure 3 shows the cyclic voltammetry results for one of the electrodes used in the study. It can be observed that the area within the hysteresis curves increased following coating. Specifically, in the representative example shown in figure 3, owing to the coating procedure, the area increased from 6.7 ± 0.6 to 39.1 ± 1.1 mC cm^{-2} for the 12 recording electrodes and from 12.8 ± 0.5 to 37.0 ± 2.3 mC cm^{-2} for the three stimulation electrodes. Therefore, the charge storage capacity (total amount of reversible charge available in the cathodic phase of the stimulation pulse) increased.

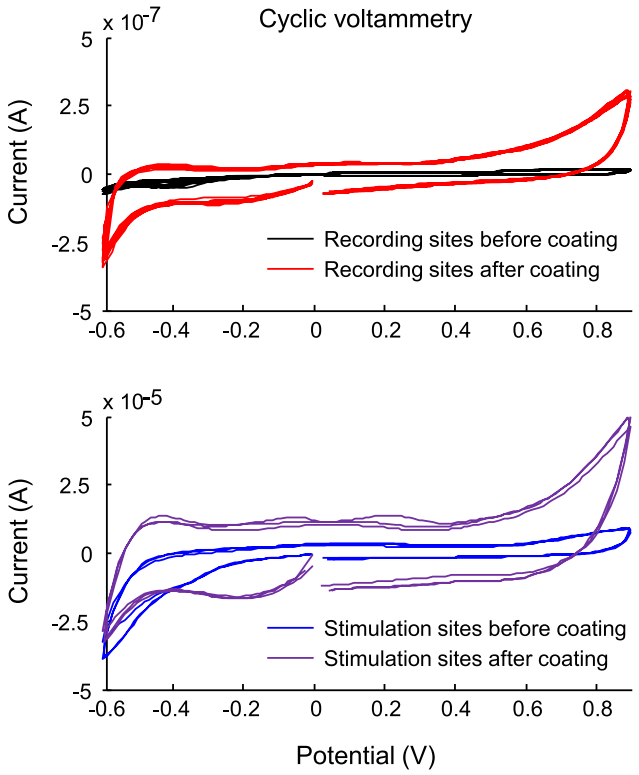

Figure 3. Representative example of the cyclic voltammetry of the 12 recording sites before (black) and after (red) coating with microrough platinum and of the three stimulation sites coated (purple) and not (blue). The area within the hysteresis curve increased following the coating procedure.

By increasing the microscopic surface area of platinum contacts with the electroplating process employed in this study, the charge injection capacity reached a value of ~500 μC cm^{-2} (Poppendieck *et al* 2009), ten times greater than the value used in the calculation of the maximal current allowed for stimulation, yielding to a further increase of the safety margin.

3.2. Results in tremor patients

Due to the insertion angle and relatively small dimension of the forearm muscles, in four out of six patients, only one stimulation channel was fully within the target muscles as assessed by the number of recording channels that contained EMG (see electrode geometry in figure 1(A)). In two patients, two stimulation channels were fully within the extensor muscle. The stimulation currents that elicited the perception threshold were 0.7 $\pm$ 0.2 mA (across six stimulation sites, range 0.4–1.0 mA) and 0.4 $\pm$ 0.2 mA (across eight stimulation sites, range 0.1–0.8 mA) for flexor and extensor muscles, respectively. The determined current limits were 1.4 $\pm$ 0.7 mA (range, 0.7–2.1 mA) for flexors and 1.5 $\pm$ 0.7 mA (0.6–2.5 mA) for extensors, always below the safety limit of the electrode contacts.

Figure 4 shows the results obtained from the feasibility test of applying the novel thin-film electrodes for tremor suppression using the system we proposed in Dosen *et al* (2015) in a PD patient. In this representative case, two stimulation channels were inside the extensor muscle, which was chosen as trigger for the out-of-phase stimulation. The perception and discomfort thresholds were 0.4 mA and 1.9 mA, respectively, and the stimulation current was set to 1.5 mA. For the flexor muscle, only one stimulation site was activated using 2 mA current (perception threshold 0.5 mA, current limit 2.5 mA, no discomfort). The patient exhibited persistent low-intensity tremor, and the system application reduced the tremor amplitude. The average suppression was 58% for the wrist angle, which is within the attenuation range reported in Dosen *et al* (2015).

3.3. Results of the sensory feedback experiment

The perception threshold and current limit for each stimulation channel for the three subjects (S1–3) are reported in table 1. Figure 5 shows the recognition performance of the three participants. For S1, the sensitivity was 64.3% and the specificity 92.8%. In this case, the shallow channel (el3) was the one with the best performance while there was some confusion between the two deep channels. When the stimulation was delivered to the deeper channels (el1 and el2), the subjects would often confuse the stimulation site (mistake el1 for el2 and vice versa) but also stimulation amplitude within the same site (e.g., mistake el2 high for el2 low). For this reason, in the remaining two subjects we considered only the superficial channel (el3) and one of the deep stimulation sites (el2). With less patterns to distinguish, the sensitivity improved to 85.7% and the specificity to 95.2% in both subjects S2 and S3. Nevertheless, the subjects exhibited similar pattern of errors by confusing the site and/or intensity when the stimulation was delivered through the deeper channel.

4. Discussion

We presented the design and manufacturing of an (acutely) implantable intramuscular electrode for multichannel recording and stimulation. The recording and stimulation contacts are embedded on the opposite sides of the substrate, leading to a compact design. The electrode is applied through a simple insertion using a hypodermic needle. We have also shown the feasibility of using this electrode in two representative neuroprosthetic applications related to tremor reduction and sensory feedback. The electrode could be safely implanted and used for both recording and stimulation.

4.1. Electrode design

A key feature of our electrode is that it can be acutely implanted with a standard hypodermic needle similar to those used in clinical EMG and removed after the experiment by simply unthreading it from the muscle. This allows to test and consequently refine the design before producing a fully implantable device. Importantly, it also allows patients to experience the performance achievable with invasive technology and decide whether it is worth to opt for an invasive solution.

The electrode is built with biocompatible material. The same material has been previously used for intraneural recording and has been safely implanted into human nerves for four weeks (Rossini *et al* 2010). The substrate is only 20

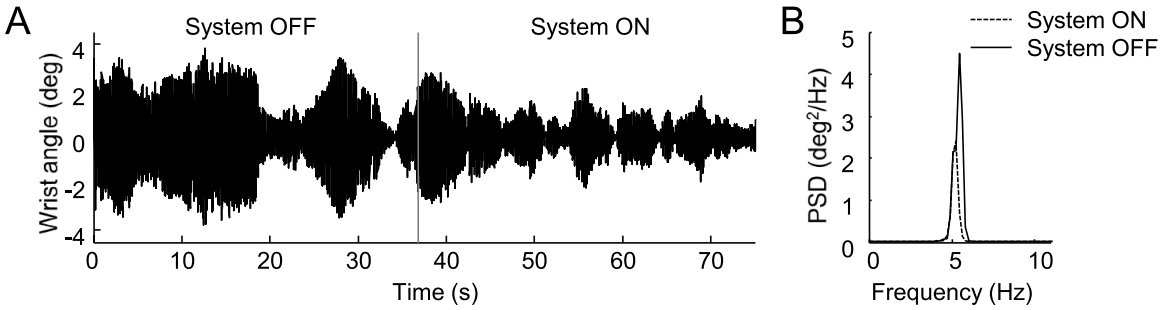

Figure 4. (A) Wrist angle recorded from a patient with Parkinson's disease during the first trial. The first portion of the signals was recorded when the tremor suppression system was OFF and was used to provide an estimation of the tremor power at baseline. The vertical grey line indicates when the system was switched ON. It can be seen that this resulted in a reduction of the tremor amplitude. (B) Power spectral density (PSD) of the wrist angle recorded during the recording and stimulation time intervals.

μm thin and conforms well with the muscle tissue. In our previous study (Muceli *et al* 2019), we showed that the detection sites are small enough to obtain selective EMG activity from the target muscle without crosstalk from neighbouring muscles (detection area of ~30 mm^2). In the present study, a large common ground was used so that the stimulation also selectively acted at the sites where the current was delivered. However, more focal stimulation could be obtained using two stimulation contacts of the electrode as cathode and anode, limiting the spatial spread of the electric field.

Differently from other invasive interfaces for recording/stimulation (Fenik *et al* 2001, Lago *et al* 2007, Rossini *et al* 2010), our electrode targeted muscles rather than nerves. The advantage is that the muscle tissue is more easily accessible and it can be regarded as an amplifier of the neural activity (Kuiken *et al* 2004). Therefore, the thin-film electrode can be used to read out efferent activity from the muscle fibers while simultaneously stimulating afferent nerve fibers. This is challenging to accomplish when using a neural electrode because the efferent and afferent fibers are intermingled and the signal to noise ratio is low.

The interface features 12 detection sites and three stimulation contacts. The high number of recording contacts provides the possibility of selecting the channel where the signal is of the best quality, as in the application of the electrode for tremor suppression. Also, given the selectivity of the recording sites, the electrode can be employed for the detection of single motor unit action potentials (Muceli *et al* 2015, 2019, Luu *et al* 2018). This can be useful in neurophysiological studies, for example in tremor patients (see e.g. Gallego *et al* (2015)), for an accurate detection of tremor oscillations (Dideriksen *et al* 2011), or for detecting efferent commands for prosthesis control (Bergmeister *et al* 2017). On the other hand, the availability of multiple stimulation contacts may be useful for selecting the stimulation sites that provide the most comfortable and/or distinguishable sensation when the electrode is used for sensory feedback, or the most effective recruitment of afferent fibers (e.g. Ia, (Dideriksen *et al* 2017)) in neuromodulation for tremor suppression. Moreover, simultaneous stimulation through multiple contacts may be employed to deliver more current if necessary. With the adopted current limit and an ample safety margin, this would not cause damage to the tissue surrounding the implant or electrode corrosion. Finally, the stimulation could be alternatively delivered to different sites to sequentially recruit different pools of afferent fibers and thereby prevent habituation (Buma *et al* 2007).

Table 1. Current corresponding to perception threshold and current limit for each of the three stimulation sites in the sensory feedback experiment. S1–3: healthy normally limbed subjects who took part in the experiment.

Subject	Site	Perception threshold (mA)	Current limit (mA)
S1	1	1.7	2.6
	2	1.1	2.6
	3	0.7	2.1
S2	2	0.3	0.8
	3	0.6	2.1
S3	2	1.6	2.4
	3	0.3	2.0

4.2. Application in tremor patients

The experiment in tremor patients mainly focused on psychometric evaluation of electrical stimulation. The stimulation current limits in tremor patients were lower than those previously observed in patients with the same pathology when using surface electrodes for stimulation (Dosen *et al* 2015, Dideriksen *et al* 2017).

In the proof of concept experiment on tremor reduction, results were similar to those previously obtained using surface electrodes (Dosen *et al* 2015). A full evaluation of the implanted version of the tremor attenuation system we proposed in Dosen *et al* (2015) goes beyond the purpose of this paper where we only aimed at showing that the recording/stimulation electrodes can be applied safely and are functional.

Only one EMG channel was used to trigger the out-of-phase stimulation in the simple approach reported in this paper. However, an abundance of channels may turn useful for improving tremor detection and consequently stimulation timing. For instance, it has been shown that motor unit spike trains may provide a better estimate of pathological tremor than surface EMG (Dideriksen *et al* 2011). This approach would require the online decomposition of multichannel intramuscular EMG recorded using the novel electrode into the constituent motor unit spike trains that could be accomplished

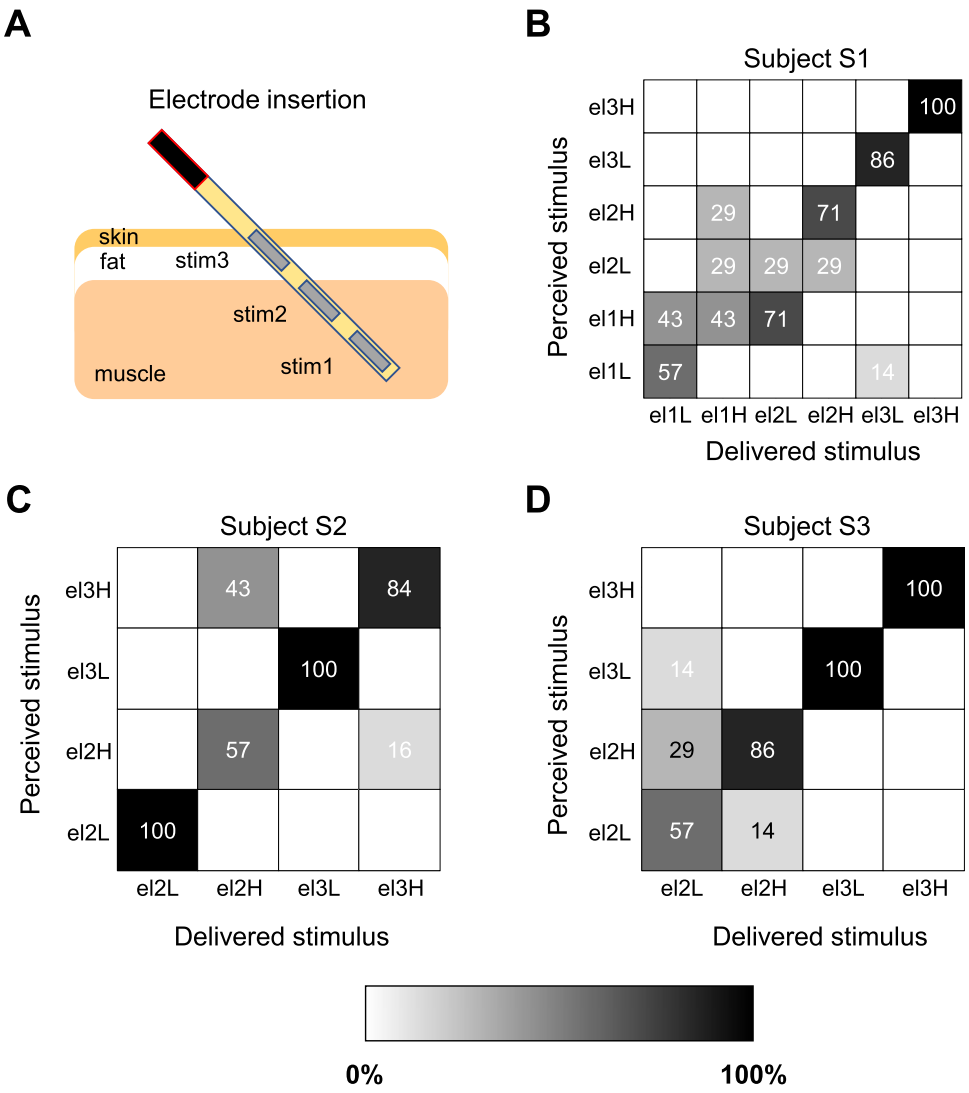

Figure 5. Setup and results of the sensory feedback experiment. (A) The double-sided thin-film electrode was inserted so that the two stimulation sites close to the electrode tip were entirely within the target muscle and the shallow one was in the skin/fat layer. (B)–(D) Confusion matrices for the stimulation pattern recognition in subjects S1-3.

by extending recently developed decomposition methods (Glaser *et al* 2013, Negro *et al* 2016, Karimimehr *et al* 2017).

4.3. Application for sensory feedback

We investigated the recognition rate when six and four stimulation patterns were presented to one and two healthy subjects, respectively. Even if the number of subjects is too small for drawing general conclusions, we have demonstrated that the stimulation contacts of the novel electrode can be indeed used to produce comfortable and yet discriminable sensations. Importantly, this is the first preliminary investigation of an electrotactile interface that is capable of generating sensations at different depths within the forearm, from the subcutaneous layer to the muscle tissue. The preliminary results show that six patterns presented in the same electrodes could not be clearly distinguished. As a general trend, stimulation in the third, most superficial electrode site could be clearly distinguished from stimulation of the two deeper sites. This may be due to the fact that the insertion depth was chosen so that the third stimulation site was close to the skin surface while the other two were within the muscle. Therefore, it is possible that different afferent fibres were activated (cutaneous for the third channel and intramuscular for the other two channels) which resulted in distinct sensations elicited by the stimulation. Also, in case of the third contact, the three subjects could clearly distinguish the two stimulation amplitudes. This may be attributed to the fact that the difference in current between the low and high amplitude stimulation was bigger than in the case of the two stimulation sites close to the electrode tip, especially for subjects S2 and S3 (see the difference between current limit and perception threshold in table 1). Despite the results were worse for the deeper electrodes, they demonstrate that sensory feedback for a myoelectric prosthesis could also employ the spatial modulation in depth, i.e. within the forearm and not only along the surface of the limb, as usually applied (Dosen *et al* 2017, Markovic *et al* 2018). In these representative examples (figure 5), we

asked the subject to recognize at least four different patterns from the same thin-film intramuscular electrode. This would not necessarily be the case in a real application when the subject will have different electrodes implanted in different muscles, e.g. if a multifunction prosthesis is operated under direct control or a pattern recognition-based control. In this scenario, for the prosthesis user it would be sufficient to recognize one pattern per electrode (e.g. corresponding to one movement in case of direct control). Still, the possibility of having more stimulation channels may be useful in order to find the stimulation site characterized by the widest range between the current limit and the perception threshold so that the stimulation amplitude may be modulated proportionally to the prosthesis displacement or velocity. In addition, increasing the number of feedback channels by distributing them throughout the forearm could be an effective method to increase the communication bandwidth of the feedback interface. The novel thin-film electrode is an ideal interface to investigate potential configurations of such a feedback system (number of channels, placement depth).

5. Conclusions

In this study we presented the design and testing of a multichannel thin-film electrode that can be used for muscle recording and stimulation. The electrode has been designed to provide an integrated interface for neuroprosthetic applications that require to gather signals from the muscle and to deliver electrical stimulation. We have shown a few representative examples of the use of the electrode for tremor suppression or for providing sensory feedback. The design of the electrode that can be acutely implanted (without surgery) and removed after the experiment is a notable feature as it allows to test the electrode and refine the design for a specific application, before producing a prototype that can be chronically implanted.

Acknowledgment

We thank Mr Bernd Müller for taking the picture used in figure 1(C).

Funding

This study was financed by the European Projects EXTEND (H2020-ICT-23-2017-779982) and NeuroTREMOR (FP7-ICT-2011-7-287739). The funding agency was not involved in the collection, analyses, and interpretation of data or writing and publication of this article.

Competing interests

The authors declare that the research was conducted in the absence of any commercial or financial relationships that could be construed as a potential conflict of interest.

ORCID iDs

Silvia Muceli https://orcid.org/0000-0002-0310-1021
Dario Farina https://orcid.org/0000-0002-7883-2697

References

Antfolk C, Alonzo M D, Rosén B, Lundborg G and Cipriani C 2013 Sensory feedback in upper limb prosthetics *Expert Rev. Med. Devices* **10** 45–54
Asghari Oskoei M and Hu H 2007 Myoelectric control systems-A survey *Biomed. Signal Process. Control* **2** 275–94
Basmajian J and Stecko G 1962 A new bipolar electrode for electromyography *J. Appl. Physiol.* **17** 849
Bergmeister K D *et al* 2017 Broadband prosthetic interfaces: combining nerve transfers and implantable multichannel EMG technology to decode spinal motor neuron activity *Frontiers Neurosci.* **11** 421
Buma D G, Buitenweg J R and Veltink P H 2007 Intermittent stimulation delays adaptation to electrocutaneous sensory feedback *IEEE Trans. Neural Syst. Rehabil. Eng.* **15** 435–41
Cipriani C, Segil J L, Birdwell J A and Weir R F 2014 Dexterous control of a prosthetic hand using fine-wire intramuscular electrodes in targeted extrinsic muscles *IEEE Trans. Neural Syst. Rehabil. Eng.* **22** 828–36
Cogan S F 2008 Neural stimulation and recording electrodes *Ann. Rev. Biomed. Eng.* **10** 275–309
Dideriksen J L, Gallego J A and Farina D 2011 Characterization of pathological tremor from motor unit spike trains *IFMBE Proc.* **34** 41–4
Dideriksen J L, Laine C M, Dosen S, Muceli S, Rocon E, Pons J L, Benito-Leon J and Farina D 2017 Electrical stimulation of afferent pathways for the suppression of pathological tremor *Frontiers Neurosci.* **11** 178
Dosen S, Markovic M, Hartmann C and Farina D 2015 Sensory feedback in prosthetics: a standardized test bench for closed-loop control *IEEE Trans. Neural Syst. Rehabil. Eng.* **23** 267–76
Dosen S, Markovic M, Strbac M, Perovic M, Kojic V, Bijelic G, Keller T and Farina D 2017 Multichannel electrotactile feedback with spatial and mixed coding for closed-loop control of grasping force in hand prostheses *IEEE Trans. Neural Syst. Rehabil. Eng.* **25** 183–95
Dosen S, Muceli S, Dideriksen J, Romero J, Rocon E, Pons J and Farina D 2015 Online tremor suppression using electromyography and low level electrical stimulation *IEEE Trans. Neural Syst. Rehabil. Eng.* **23** 385–95
Fenik V, Fenik P and Kubin L 2001 A simple cuff electrode for nerve recording and stimulation in acute experiments on small animals *J. Neurosci. Methods* **106** 147–51
Gallego J A, Dideriksen J L, Holobar A, Ibanez J, Glaser V, Romero J P, Benito-Leon J, Pons J L, Rocon E and Farina D 2015 The phase difference between neural drives to antagonist muscles in essential tremor is associated with the relative strength of supraspinal and afferent input *J. Neurosci.* **35** 8925–37
Gallego J A, Rocon E, Belda J M and Pons J L 2013 A neuroprosthesis for tremor management through the control of muscle co-contraction *J. Neuroeng. Rehabil.* **10** 36
Glaser V, Holobar A and Zazula D 2013 Real-time motor unit identification from high-density surface EMG *IEEE Trans. Neural Syst. Rehabil. Eng.* **21** 949–58
Graczyk E L, Schiefer M A, Saal H P, Delhaye B P, Bensmaia S J and Tyler D J 2016 The neural basis of perceived intensity in natural and artificial touch *Sci. Transl. Med.* **8** 362ra142
Guo L, Kitashima L J, Villari C R, Klein A M and DeWeerth S P 2009 Muscle surface recording and stimulation using

integrated pdms-based microelectrode arrays: recording-triggered stimulation for prosthetic purposes *2009 IEEE Biomedical Circuits and Systems Conf. BioCAS 2009* pp 101–4
Guvanasen G S, Aguilar R, Guo L, Karnati C, Rajaraman S, Nichols T R and Deweerth S P 2017 Stretchable, microneedle electrode array for measuring intramuscular electromyographic activity *IEEE Trans. Neural Syst. Rehabil. Eng.* **25** 1440–52
Heuschkel M O, Fejtl M, Raggenbass M, Bertrand D and Renaud P 2002 A three-dimensional multi-electrode array for multi-site stimulation and recording in acute brain slices *J. Neurosci. Methods* **114** 135–48
Karimimehr S, Marateb H R, Muceli S, Mansourian M, Mañanas M A and Farina D 2017 A real-time method for decoding the neural drive to muscles using single-channel intramuscular EMG Recordings *Int. J. Neural Syst.* **27** 1750025
Kingdom F A A and Prins N 2009 *Psychophysics: a Practical Introduction* (New York: Academic)
Kuiken T A, Dumanian G A, Lipschutz R D, Miller L A and Stubblefield K A 2004 The use of targeted muscle reinnervation for improved myoelectric prosthesis control in a bilateral shoulder disarticulation amputee *Prosthet. Orth. Int.* **28** 245–53
Lago N, Yoshida K, Koch K P and Navarro X 2007 Assessment of biocompatibility of chronically implanted polyimide and platinum intrafascicular electrodes *IEEE Trans. Biomed. Eng.* **54** 281–90
Luu B L, Muceli S, Saboisky J P, Farina D, Héroux M E, Bilston L E, Gandevia S C and Butler J E 2018 Motor unit territories in human genioglossus estimated with multichannel intramuscular electrodes *J. Appl. Physiol.* **124** 664–71
Markovic M, Schweisfurth M A, Engels L F, Bentz T, Wüstefeld D, Farina D and Dosen S 2018 The clinical relevance of advanced artificial feedback in the control of a multi-functional myoelectric prosthesis *J. Neuroeng. Rehabil.* **15** 28
Maynard E M, Nordhausen C T and Normann R A 1997 The Utah intracortical electrode array: a recording structure for potential brain-computer interfaces *Electroencephal. Clin. Neurophysiol.* **102** 228–39
Meyer J U, Stieglitz T, Scholz O, Haberer W and Beutel H 2001 High density interconnects and flexible hybrid assemblies for active biomedical implants *IEEE Trans. Adv. Packag.* **24** 366–74
Muceli S, Bergmeister K D, Hoffmann K-P, Aman M, Vujaklija I, Aszmann O and Farina D 2019 Decoding motor neuron activity from epimysial thin-film electrode recordings following targeted muscle reinnervation *J. Neural Eng.* **16** 016010
Muceli S, Poppendieck W, Negro F, Yoshida K, Hoffmann K P, Butler J E, Gandevia S C and Farina D 2015 Accurate and representative decoding of the neural drive to muscles in humans with multi-channel intramuscular thin-film electrodes *J. Physiol.* **593** 3789–804
Negro F, Muceli S, Castronovo A M, Holobar A and Farina D 2016 Multi-channel intramuscular and surface EMG decomposition by convolutive blind source separation *J. Neural Eng.* **13** 026027
Poppendieck W, Koch K P, Steltenkamp S and Hoffmann K-P 2009 A measurement set-up to determine the charge injection capacity of neural microelectrodes *Proc. 11th World Congress on Medical Physics and Biomedical Engineering* pp 162–5
Poppendieck W, Sossalla A, Krob M O, Welsch C, Nguyen T A K, Gong W, DiGiovanna J, Micera S, Merfeld D M and Hoffmann K P 2014 Development, manufacturing and application of double-sided flexible implantable microelectrodes *Biomed. Microdevices* **16** 837–50
Prochazka A, Elek J and Javidan M 1992 Attenuation of pathological tremors by functional electrical stimulation. I: method *Ann. Biomed. Eng.* **20** 205–24
Raspopovic S *et al* 2014 Restoring natural sensory feedback in real-time bidirectional hand prostheses *Sci. Transl. Med.* **6** 222ra19
Rose T L and Robblee L S 1990 Electrical stimulation with Pt electrodes. VIII. Electrochemically safe charge injection limits with 0.2 ms pulses *IEEE Trans. Biomed. Eng.* **37** 1118–20
Rossini P M *et al* 2010 Double nerve intraneural interface implant on a human amputee for robotic hand control *Clin. Neurophysiol.* **121** 777–83
Štrbac M *et al* 2016 Integrated and flexible multichannel interface for electrotactile stimulation *J. Neural Eng.* **13** 046014
Vrabec T, Bhadra N, Wainright J, Bhadra N, Franke M and Kilgore K 2016 Characterization of high capacitance electrodes for the application of direct current electrical nerve block *Med. Biol. Eng. Comput.*. **54** 191–203